Expected Performance of Fibre Multi-Object Spectrograph (FMOS): Estimation with Spectrum Simulator

Naoyuki Tamura

Department of Physics, University of Durham, South Road, Durham, DH1 3LE, UK
naoyuki.tamura@durham.ac.uk

Abstract

In this article, the simulations of spectra expected with Fibre Multi-Object Spectrograph (FMOS) are discussed. Emission and absorption lines are simulated over the spectral coverage of FMOS and how successfully fluxes, centres, and widths of those lines can be measured is investigated. Based on these calculations, the guidelines of detection limits are shown. Finally things which are not taken into account in the simulators and future perspectives of the simulators are briefly mentioned.

1. INTRODUCTION

FMOS will be capable of getting spectra at wavelengths from 0.9 to 1.8 μm, with either of the two spectral resolutions: $R \sim 500$ (Low resolution mode) and $R \sim 2200$ (High resolution mode) ("LR mode" and "HR mode" hereafter). Predicting the performance of FMOS is not as straightforward as, e.g., optical spectrographs, because of the bright OH airglow emission lines from the sky and the mechanism to suppress them in the spectrograph. In order to investigate detection limits of emission and absorption lines and how successfully line fluxes, line centres, and line widths can be measured from the spectra, it is important to develop some tools to visualise the expected performance of FMOS as spectra. We constructed two types of spectrum simulators. One is the web-based calculator (http://elvira.phyaig.dur.ac.uk/naoyuki.tamura/simulator.html). This simulates a fully reduced and calibrated spectrum according to selection of template spectrum and observing conditions. This tool is expected to be useful for a quick look at feasibility of an observing program. Another is the image simulator. This creates mock data in FITS format, including those for flat-fielding and wavelength calibrations. Thus one can try a whole process of reduction and calibration to make a final product. In the next section, the flow of calculations to simulate spectra is briefly reviewed.

2. INSIDE THE SIMULATORS

In Figure 1, the information taken into account in the simulators until the light from sky arrives onto the detector is summarised. Firstly, the light goes through the atmosphere, which has transmittance as a function of wavelength and also glows in itself. At the prime focus of the telescope, some fraction of the energy from the object gets into a fibre configured at the focal plane. Then the light goes through the subsequent optics which lead to energy loss due to internal absorption and surface reflection. Figure 2 shows the system throughput including from the atmosphere to the detector, which shows that ~ 10 % (LR mode) or ~ 20 % (HR mode) remains available after all the way through[1]. Although the effects of the OH suppression masks and the energy loss due to the aperture defined by the fibre are not allowed for in this throughput curve, they are taken into account in simulating spectra.
The next things to do are to compare the signal with the noise and to make a noisy spectrum artificially. The web-based calculator simply fluctuates the input spectrum of an object based on a signal-to-noise ratio per pixel. In the image simulator, the total number of electrons produced by incoming photons from object and sky background, dark current and so on are counted in each pixel and Poisson noise is added to the count of the stored electrons. In producing mock data in FITS format, spectrum bending and PSF variation on the detector can be taken into account and their effects on the reduction procedure can be investigated. This is performed for calibration exposures (lamps for flat-field and arc) as well as for science exposures. The details of the image simulator are described in the other contribution (Akiyama, this proceeding).

3. SIMULATIONS

3.1 LR Mode

In the following, simulated spectra in the LR mode are shown. The spectra were produced with the image simulator and the mock data were fully reduced with IRAF. As observing conditions, $0\farcs5$ seeing and a

[1]HR mode has a higher throughput than LR mode because a Volume-Phase Holographic (VPH) grating is inserted to anti-disperse a spectrum not in HR mode but in LR mode.

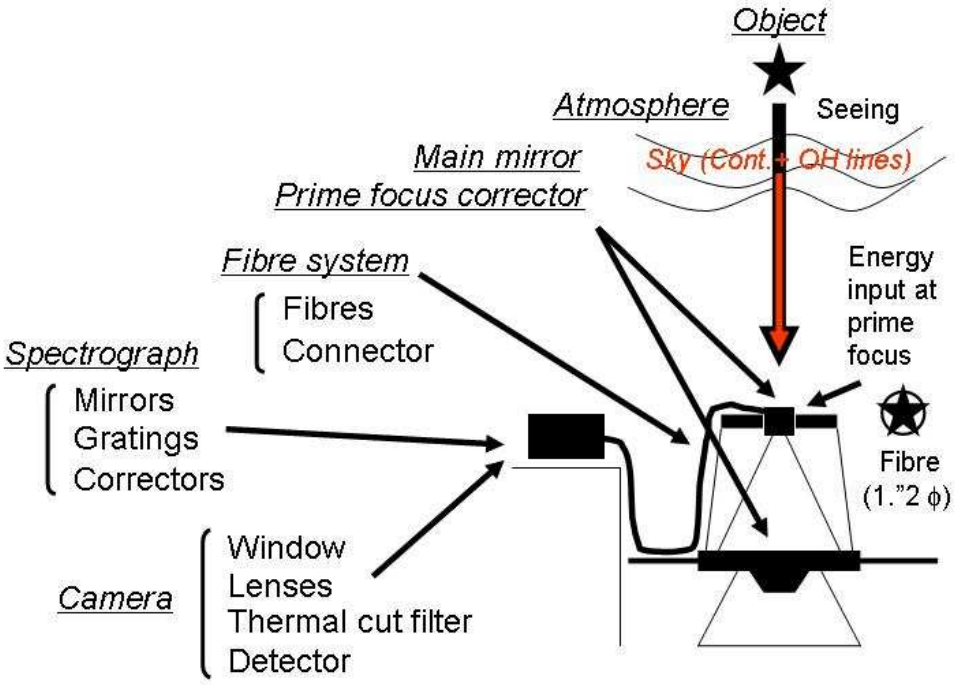

Figure 1: Schematic view of the light path from the atmosphere to the detector and the components involved on the way.

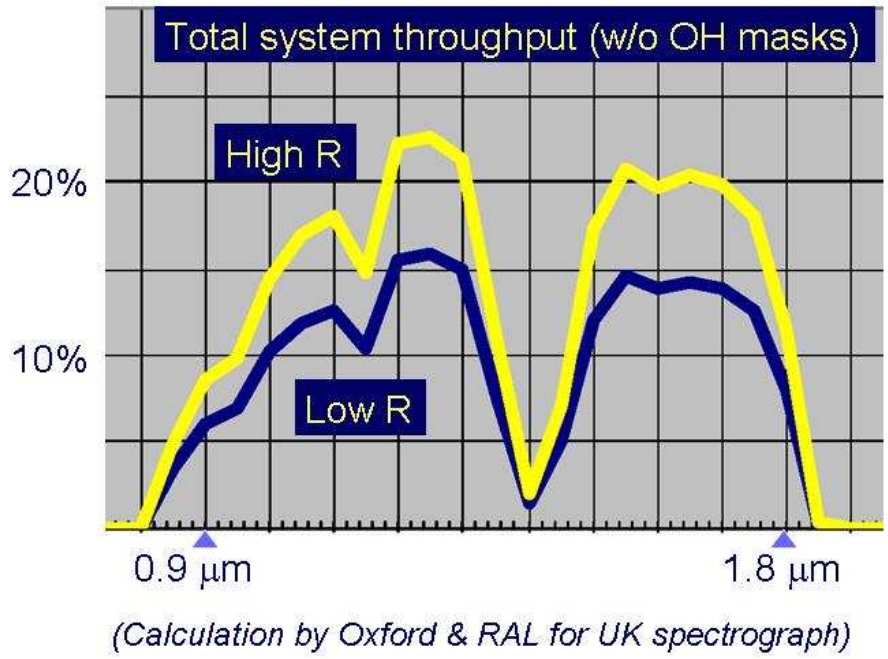

Figure 2: Total system throughput including the atmospheric absorption is shown as a function of wavelength for LR mode and HR mode. Note that this does not take into account energy loss due to the OH masks or the aperture defined by the fibre at the prime focus.

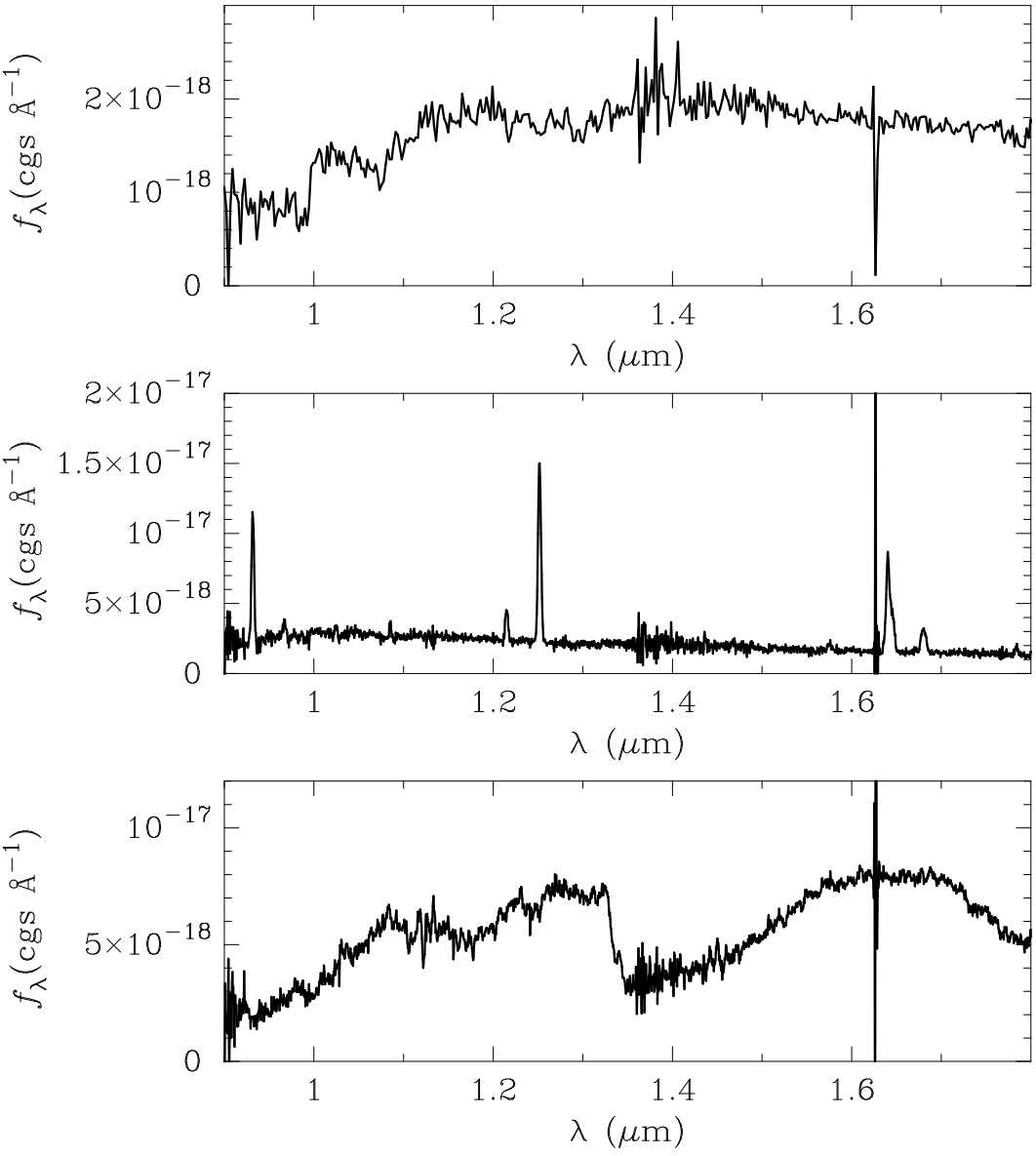

Figure 3: Simulated spectra of astronomical objects: (*Top*) An old stellar population at a redshift of 1.5 with $H = 19.5$ mag. 5 pixel binning was performed. (*Middle*) A starburst galaxy at a redshift of 1.5 with $H = 19.5$. No pixel binning was performed. (*Bottom*) An L-type dwarf star with an $H = 18.0$ mag. No pixel binning was performed.

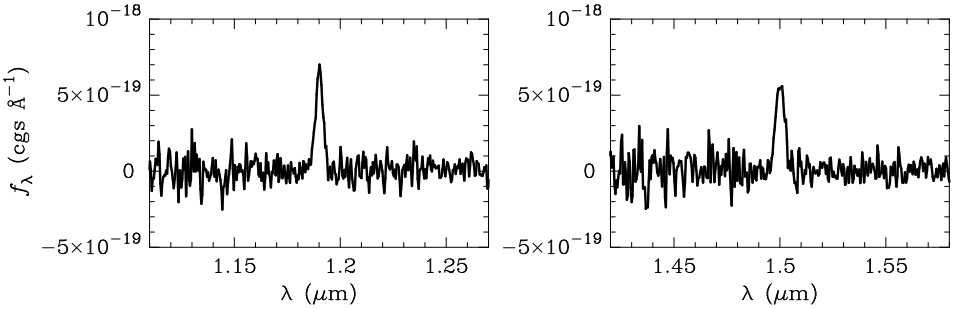

Figure 4: Simulated emission lines at two different wavelengths. The emission line flux is 6.0×10^{-17} erg cm^{-2} s^{-1} and no pixel binning was performed. See text for more details.

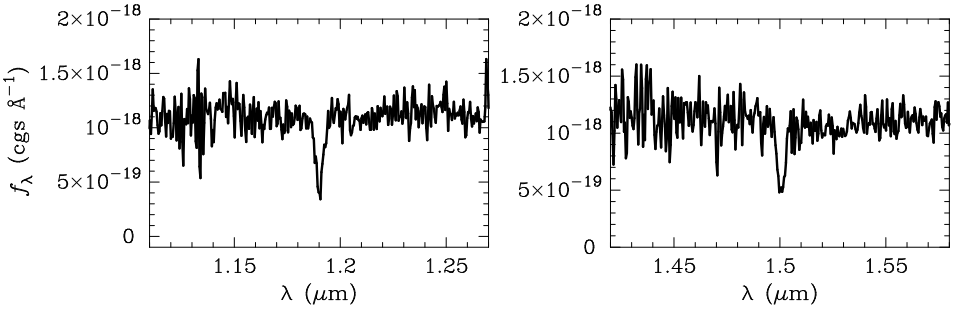

Figure 5: Simulated absorption lines at two different wavelengths. A flat continnum with the flux density of 1.1×10^{-18} erg cm^{-2} s^{-1} Å^{-1} is given, and the absorption line flux is 3.0×10^{-17} erg cm^{-2} s^{-1}. No pixel binning was performed. See text for more details.

zenith distance of about 50° (sec $z = 1.5$) were assumed for all the data. 1 hour on-source integration is also assumed. At first, some spectra of astronomical objects are presented in Figure 3: an old stellar population at a redshift of 1.5, a starburst galaxy at a redshift of 1.5, and an L-type dwarf star are shown in the top, middle, and bottom panel, respectively. Note that these are fully calibrated spectra.

Now, simulated emission lines are investigated in detail. Figure 4 shows two close-ups of simulated emission lines at 1.19 μm and 1.50 μm both of which have a line flux of 6.0×10^{-17} erg cm^{-2} s^{-1} and a line width of 300 km s^{-1}. The line profile is assumed to be a Gaussian. No continuum is assumed in this spectrum, which is also the case for all the simulated emission lines in the following. Although the lines in Figure 4 are likely to be detected with high significances, we need to keep in mind that the noise level and thus detection limit should be a function of wavelength. For example, it may be very hard to study lines around the wavelengths of the OH suppression masks. In order to investigate this wavelength dependence, an emission line was simulated at every angstrom across the spectral coverage ($0.9 \sim 1.8$ μm) and the same simulation was repeated 20 times at each angstrom. In each simulated spectrum, a line flux, line centre, and line width were measured and were compared with the given values. Figure 6 shows the results of the realisations. Here, the ratio of a measured line flux to the given value, the difference between a measured line centre and the given value, and the ratio of a measured line width to the given value is plotted against wavelength in the panel (a), (b), and (c), respectively. Note that one realisation results in one data point in each panel. In all of these panels, darker regions show the regions where data points are more crowded. The top, middle and bottom red lines in each panel show the 90 percentile, median, and 10 percentile of the distribution of the data around a wavelength within a width of 0.01 μm, respectively.

The region between 1.3 μm and 1.4 μm is noisy because of the serious atmospheric absorption band. Also, a number of vertical linear features are seen across the spectral coverage. These show the regions where the densities of the OH suppression masks are relatively high. The extremely noisy part around 1.6 μm is due to a cluster of the OH masks. Considering that the top and bottom red lines are quite close to the edges of the distribution, these plots suggest that the effects of the OH masks do not result in significant decrease of the spectral coverage.

The same realisations were performed for a few emission line fluxes and the results are summarised in Figure 7. Each data point represents the median of the distribution of the data from all the realisations for one emission line flux. The upper and lower ends of an error bar indicate the 90 percentile and 10

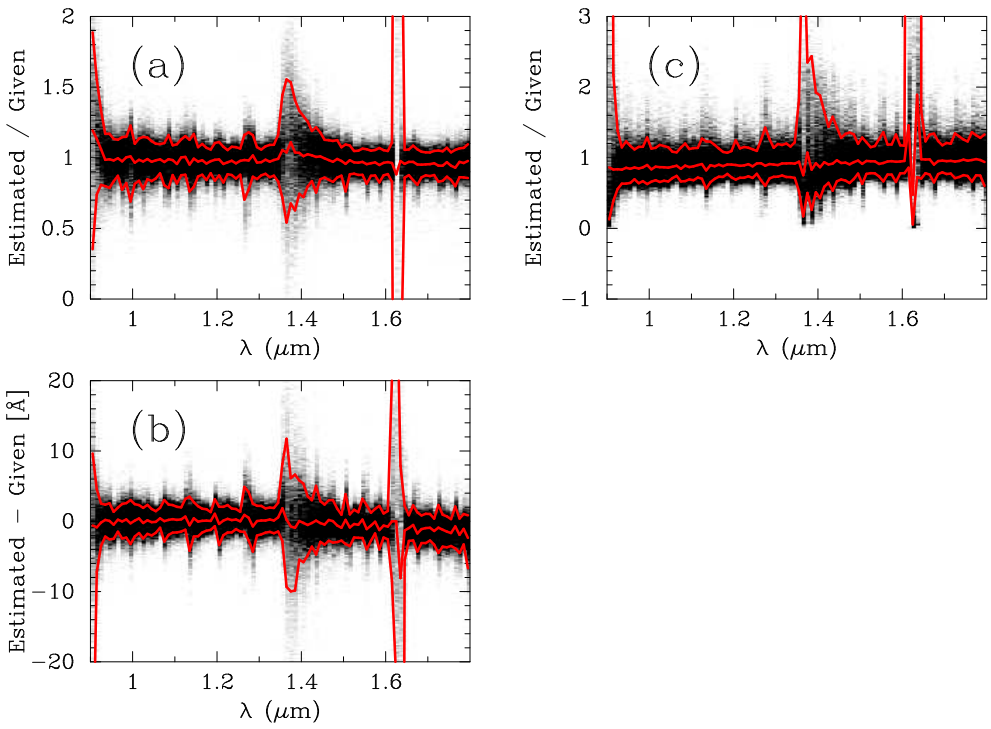

Figure 6: The results of the realisations for an emission line flux of 6.0×10^{-17} erg cm^{-2} s^{-1} in LR mode are shown: (a) ratio of measured line flux to given value, (b) difference between measured line centre and given value, and (c) ratio of measured line width to given value is plotted against wavelength. Three red lines show the 90 percentile (top), median (middle), 10 percentile (bottom) of the distribution of the data at each wavelength.

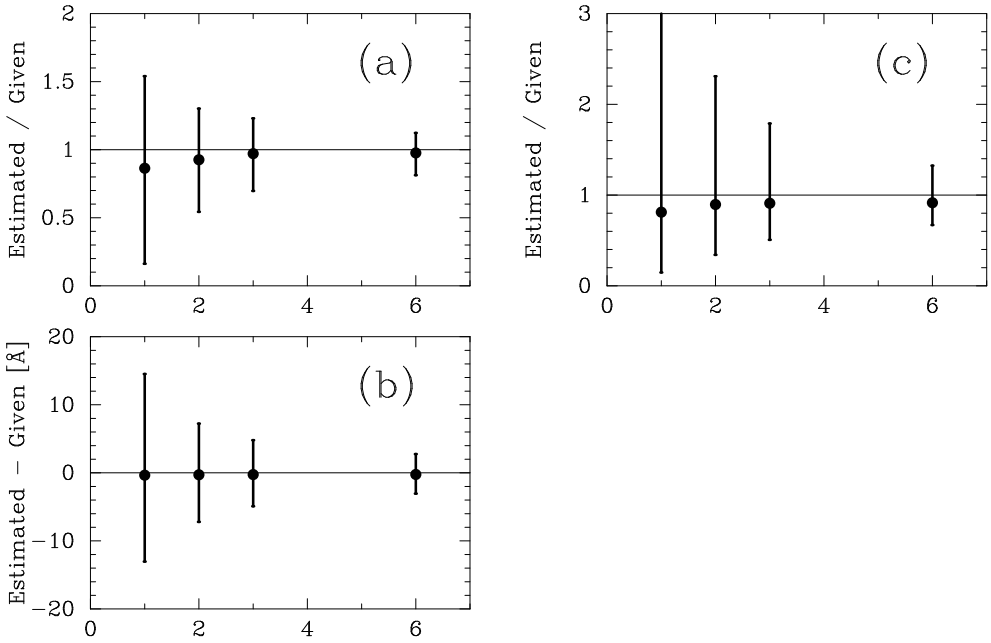

Figure 7: A summary of the realisations for a few emission line fluxes. Flux of emission line is shown in the horizontal axis in unit of 1.0×10^{-17} erg s^{-1} cm^{-2}. See text for details.

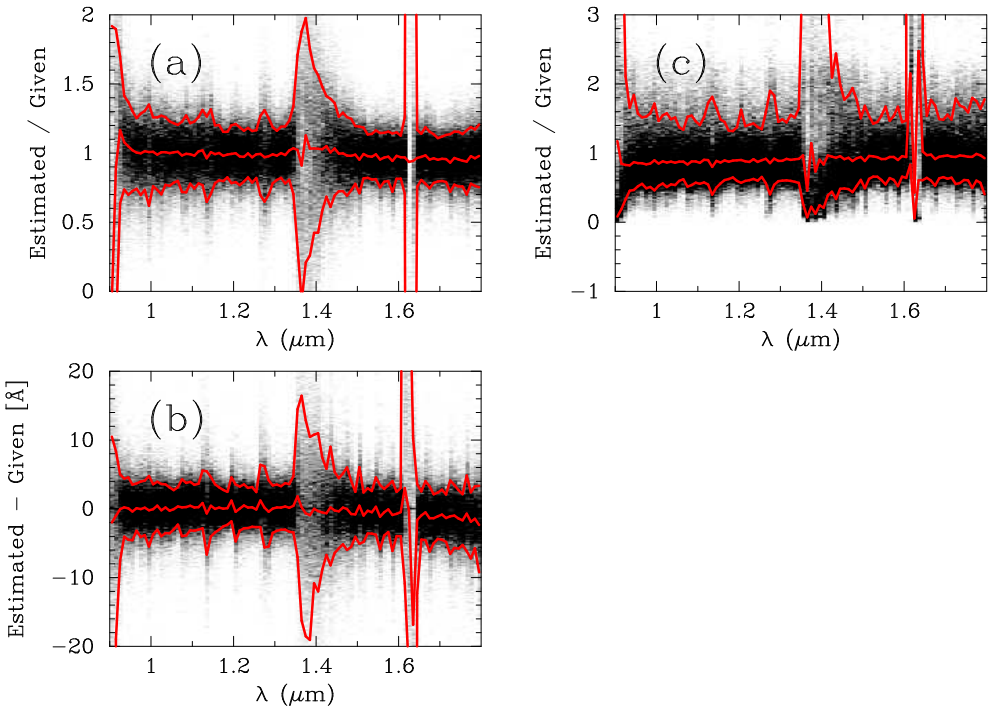

Figure 8: Same as Figure 6, but for the absorption line.

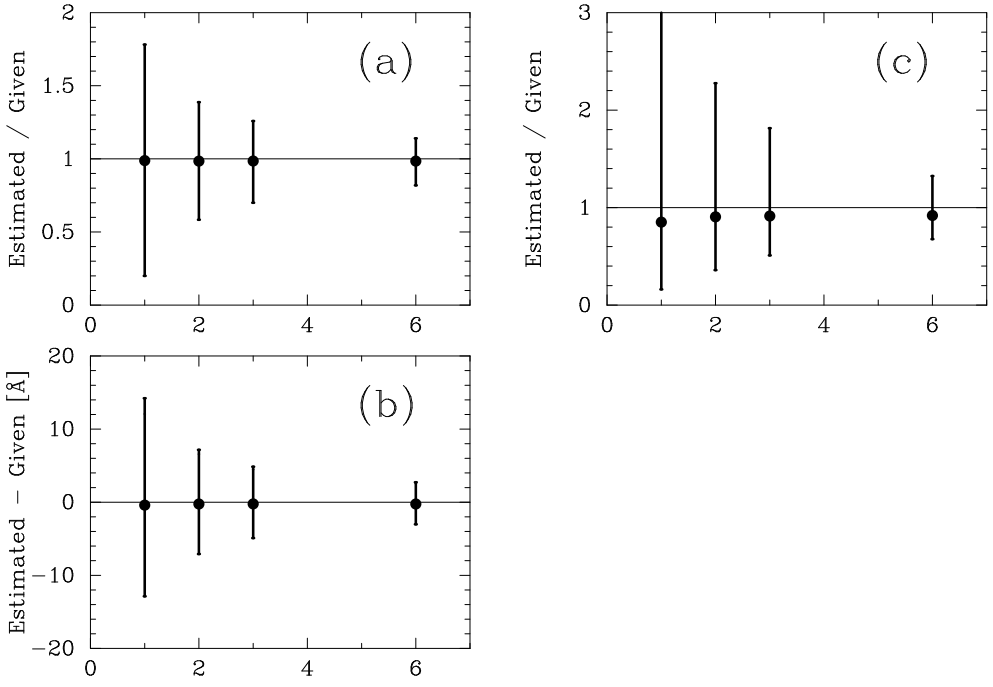

Figure 9: A summary of the realisations for a few absorption line fluxes. See text for details.

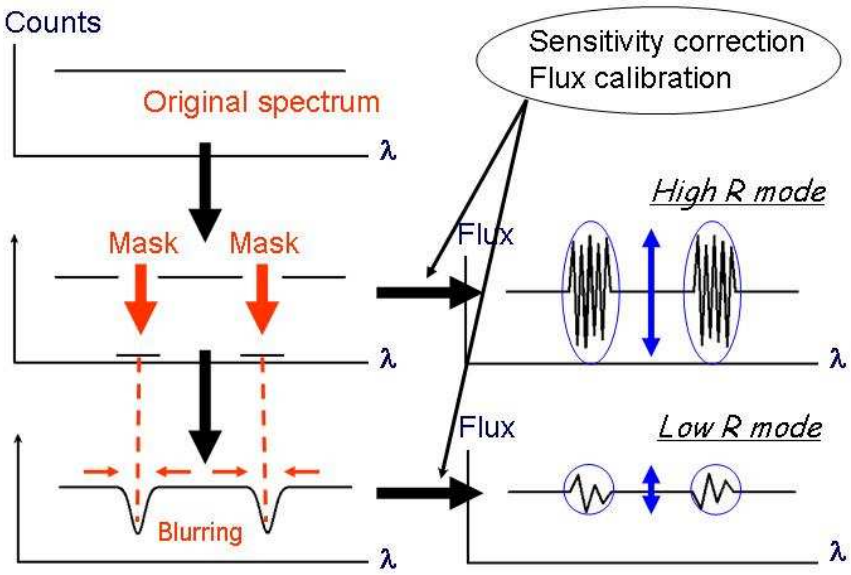

Figure 10: Schematic diagram to show the difference of the mask effects between in the LR and HR modes.

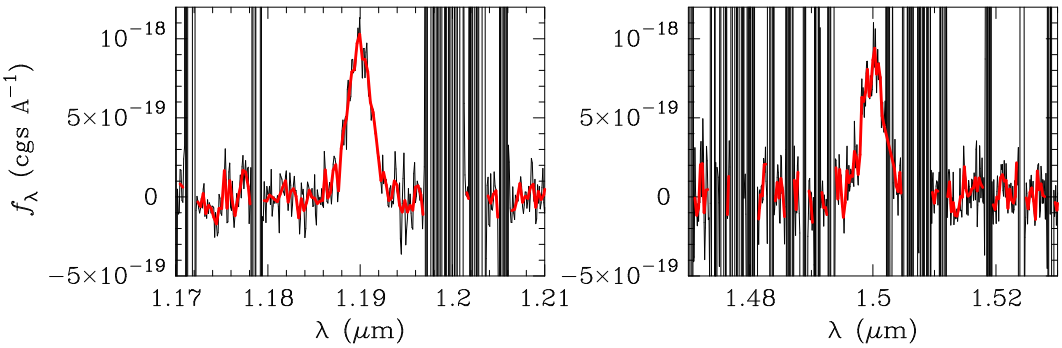

Figure 11: Same as Figure 6, but for the HR mode.

percentile of the distribution, respectively. These plots suggest that even for an emission line flux of a few times 10^{-17} erg cm^{-2} s^{-1}, it can be still detected at $\sim 3\sigma$ level in most of the spectral coverage. The detectability of absorption line was also investigated in the same way. Now a flat continuum ($f_\lambda =$ *const.*) at the level of 1.1×10^{-18} erg cm^{-2} s^{-1} Å^{-1}, which corresponds to 20 mag in H band in Vega system, is assumed. An absorption line flux is assumed to be 3.0×10^{-17} erg cm^{-2} s^{-1}. A Gaussian line profile with a width of 300 km s^{-1} is assumed. The close-ups of the absorption lines at 1.19 μm and 1.50 μm are shown in Figure 5 and the results of the realisations for this absorption line flux is indicated in Figure 8. The summary for a few absorption line fluxes is shown in Figure 9. These suggest that an absorption line flux of a few times 10^{-17} erg cm^{-2} s^{-1} can be detected for that continuum level.

3.2 HR Mode

Before showing simulated expected in the HR mode, the expected difference of the mask effect on a spectrum between in the LR and HR modes are briefly reviewed in Figure 10. In the spectrograph of FMOS, a spectrum forms on the mask mirror at first and the spectral elements at wavelengths with strong sky emissions are masked out (the middle left panel in Figure 10). Therefore, these masked regions lose nearly all the signals. In the LR mode, the spectrum on the mask mirror is anti-dispersed afterwards, which is more or less equivalent to image blurring, and thus some photons leak into the masked region from the neighboring spectral elements (the bottom left panel). This means that the noise levels in the masked spectral elements are suppressed at the expense of spectral resolution (the bottom right panel). On the other hand, in the HR mode, the spectrum on the mask mirror is rather directly transfered onto

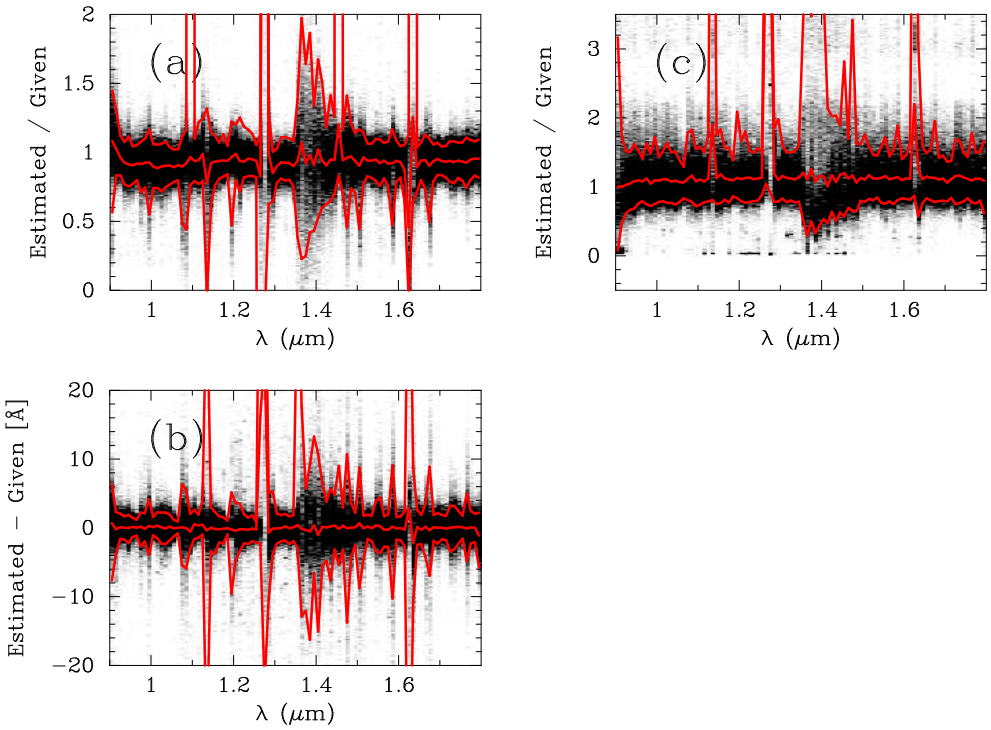

Figure 12: Same as Figure 6, but for the HR mode.

the detector. Therefore, while the spectral resolution is preserved, the regions with nearly no signal become very noisy and thus the mask effects are expected to stand out a lot more than in LR mode (the middle right panel).

In Figure 11, simulated emission lines in the HR mode are shown. The regions filled up with vertical lines show wavelengths with masks and they are unlikely to provide meaningful information. However, it should be mentioned that an individual mask is not very broad (the width corresponds to $\sim$ 150 km s^{-1} in velocity). Therefore, if a line in the spectrum of an object is broad enough (this is the case for, e.g., massive galaxies and AGN) and it falls onto a wavelength around which the OH masks are not that crowded, some interpolation techniques are likely to well recover the spectral information. In Figure 12, the results from the realisations in the HR mode for the emission line with a flux of 6.0×10^{-17} erg cm^{-2} s^{-1} and a width of 300 km s^{-1} are shown. While only a simple interpolation technique was employed to avoid the masked regions in a spectrum in measuring the line fluxes etc, the mask effects seem to have been suppressed down to a similar level to those seen in the LR mode across most of the spectral coverage (see Figure 6). This is expected to be improved with a more elaborated interpolation algorithm exploiting the fact that all the locations of the masks are known.

3. SUMMARY AND DISCUSSION

In order to visualise the expected performance of FMOS as spectra, we made two tools to simulate spectra expected from FMOS. One is the web-based calculator for quick look of feasibility, and another is the image simulator for more detailed tests including reduction and calibration methods. We simulated emission and absorption lines and investigated how successfully the information on the lines can be extracted from the spectra, assuming 1 hour on-source integration and the observing conditions of 0.″5 seeing and $\sec z = 1.5$. Although the results slightly depend on wavelength and observing mode (i.e., spectral resolution), the following numbers can be guidelines of significance of the line detection: For the emission line with a flux of 6.0×10^{-17} erg cm^{-2} s^{-1} and without continuum, the line flux, line centre, and line width can be estimated within an accuracy of 10 %, 5 Å, and 20 % respectively. The same numbers can be applied to the absorption line with an absorbed flux of 3.0×10^{-17} erg cm^{-2} s^{-1} on the flat continuum at the level of 1.1×10^{-18} erg cm^{-2} s^{-1} Å^{-1} ($H = 20$ mag).

One important caution is that those estimated uncertainties do not include any calibration errors. It is unrealistic to observe a standard star with each fibre in an observing run and thus, generally speaking, precise flux calibration (i.e., spectrophotometry) is not highly expected with multi-object fibre spectroscopy. Also, well-behavioured sky is assumed and sky subtraction is assumed to be performed ideally

at this moment, which can be an optimistic assumption. However, with regard to sky subtraction, assigning several fibres to look at sky in the vicinity of an object could allow us to get enough accuracy of sky subtraction even for faint objects. Nevertheless it may be worth trying to model possible errors in sky subtraction in the simulators. In addition, because of the OH masks, errors in flat-fielding and wavelength calibration may interplay to make some artificial features in spectra, which have not taken into account in any simulations yet. However it is stressed that the spectrographs for FMOS are bench-mounted and will be more stable than, e.g., the 2dF spectrograph and thus such errors are less likely to occur.